Original Article

Effect of Sodium Hypochlorite Inhalation on the Structure of Tracheal Mucosa in Adult Male Albino Rats and the Possible Reversibility upon Recovery

Mary Refaat Isaac, Hagar Yousry Rady and Shereen Adel Saad

Department of Anatomy and Embryology, Faculty of Medicine, Ain Shams University, Egypt

ABSTRACT

Introduction: The worldwide COVID-19 pandemic has led to wide usage of disinfectants as Sodium hypochlorite (NaOCL). Some studies declared that exposure to chlorine-based disinfectants is considered as a source of irritation and airway inflammation.

Aim of Work: Determine the histopathological effects of NaOCL inhalation on the tracheal mucosa and the reversibility of these effects upon recovery.

Material and Methods: Forty adult male albino rats were divided into three groups. Group I: was further subdivided into subgroup IA: ten rats were used as negative control, subgroup IB: ten rats exposed to nebulized distilled water 20 minutes/day for three weeks. Group II: ten rats exposed to nebulized 4% NaOCL 20 minutes/day for three weeks. Group III: ten rats exposed to NaOCL same as group II and were left for another three weeks without exposure. At the end of experiment for each group, rats were anesthetized, sacrificed and trachea were excised and processed for light and electron microscopic examination also morphometric and statistical studies were done.

Results: Examination of sections of group II rats revealed marked distortion of tracheal epithelial cells, indistinct cell boundaries, shrunken heterochromatic nuclei, loss of apical cilia and highly significant decrease in epithelial height with highly significant increase in mean of number of goblet cells and area percentage of collagen. Sections of the group III showed that the tracheal lining was almost restored. Yet, it appeared disorganized cells, with restored but almost amalgamated cilia. Goblet cells revealed back to normal number but were still variable shaped. However, mean epithelial height and mean area percentage of collagen did not go back to their control ranges.

Conclusion: Inhalation of NaOCL has been found to cause partially reversible histopathological effects on the tracheal mucosal. Thus, excessive use of household chlorine containing detergents should be limited or better substituted by others.

Received: 23 February 2022, **Accepted:** 24 March 2022

Key Words: Recovery, sodium hypochlorite, trachea.

Corresponding Author: Mary Refaat Isaac, PhD, DDepartment of Anatomy and Embryology, Faculty of Medicine, Ain Shams University, Egypt, **Tel.**: +20 10 0117 1964, **E-mail:** drmaryrefaat@yahoo.com

ISSN: 1110-0559, Vol. 46, No. 3

INTRODUCTION

The worldwide pandemic of coronavirus (COVID-19) has led to wide usage of disinfectants to sterilize surfaces and buildings[1] as transmission of the COVID-19 virus has been reported to be linked to contaminated environmental surfaces[2].

Among the various household cleaning product, sodium hypochlorite (NaOCL) (3-6%) is one of the most common disinfectants used due to its low cost and wide range of antimicrobial activity[3]. It has been proven to be effective against several common pathogens at various concentrations[4]. Unfortunately, when NaOCL is mixed with water, highly reactive chemicals are produced as chlorine gas, hypochlorous acid and hydrochloric acid[5].

Chlorine gas is a reactive oxidant gas[6], and when inhaled, it is dissolved in the epithelial lining fluid and either generates hypochlorous and hydrochloric acids or reacts rapidly with molecules in the epithelial lining fluid[7]. Moreover, hydrochloric and hypochlorous acids generate superoxide radicals that cause oxidative injury and cell death[8].

Some studies declared that the exposure to chlorine-based disinfectants is considered as a source of irritation and airway inflammation[9]. It has been declared that inhalation of chlorine gas affects the epithelium of both upper and lower airways, leading to pulmonary dysfunction[10].

Thus, the aim of this study was to determine the histopathological effects of NaOCL inhalation on the tracheal epithelium of adult male albino rats and the reversibility of these effects upon recovery.

MATERIAL AND METHODS

Drugs

Sodium hypochlorite

A mixture of 4% sodium hypochlorite dissolved in distilled water[5] was put in a nebulizer (Norditali Elettromedicali S.R.L–25010 S. Martino della Battaglia – Italy) to deliver the aerosol at a rate of 0.25 ml/min. Rats were nebulized for 20 minutes daily for three weeks[5].

 DOI: 10.21608/ejh.2022.123544.1643

Animals

Forty male adult albino rats weighing 200 - 220 gm were obtained from the animal house of the Faculty of Medicine Ain Shams Research Institute (MASRI). Rats were kept in ordinary wire-mesh cages in a room temperature (21±3 ℃). They were provided standard rat diet and granted free access to water. They were housed for a week preceding the experiment in order to accommodate to the experimental conditions. This experiment followed the guidelines of the Committee of the Animal Research Ethics (CARE) at Faculty of Medicine, Ain Shams University.

Experimental Protocol

Animals were divided into three groups as follows:

Group I (control group): It was further equally subdivided into:

- Subgroup IA: composed of ten rats that were not exposed to anything and were used as negative control.
- Subgroup IB: composed of ten rats that were exposed to nebulized distilled water for 20 minutes every day for three weeks.

Group II (NaOCL inhalation group): Ten adult rats were exposed to nebulized 4 % NaOCL, for 20 minutes every day for three weeks.

Group III (Recovery group): Ten adult rats were exposed to nebulized 4 % NaOCL, for 20 minutes every day for three weeks, then were left another three weeks without exposure.

At the end of experiment for each group, rats were anesthetized using intraperitoneal injection of thiopental sodium and then sacrificed. Trachea was excised and middle one third was cut longitudinally into two halves.

Histological techniques

One half was fixed in 10% neutral-buffered formalin, dehydrated, then embedded in paraffin blocks. Sections of 5µm thickness were subsequently cut and stained with hematoxylin and Eosin (H&E) and Masson Trichrome stains.[11]

The other half was cut in 1mm3 thick parts, fixed in 4% glutaraldehyde to be processed for transmission electron microscopic examination. Semithin sections were stained with Toluidine blue and examined by the light microscope. The ultrathin sections from selected fields were stained with Uranyl Acetate and Lead Citrate[12], examined and photographed by Philips 201- transmission electron microscope of Electron Microscope Unit, Faculty of Science - Ain Shams University.

Morphometric studies

The height of the tracheal epithelium and number of goblet cells were measured in H&E-stained sections. The area percentage of collagen fibers was also measured in Masson trichrome stained sections. Measurements were done in randomly chosen five fields/section in five different sections for every rat in each group at magnification x400 using image analyser Leica Q win V.3 program installed on a computer in the Histology Department, Faculty of Medicine, Ain Shams University. The computer was connected to a Leica DM2500 microscope (Wetzlar, Germany).

Statistical analysis

Mean epithelial height and mean goblet cell number in H&E-stained sections and mean area percentage of collagen fibers in Masson Trichrome stained sections of each rat in each group were collected. Data analysis was performed using Microsoft Office Excel 356 (Microsoft, USA). Analyses of Variance (ANOVA test) and student t-test were done and data were presented as mean ± standard deviation (SD) and were considered highly significant when $P \leq 0.001$, significant when $P \leq 0.05$ and insignificant when $P > 0.05$.

RESULTS

Examination of sections of subgroups IA and IB revealed almost similar histological picture. Hematoxylin and eosin-stained sections showed that the tracheal mucosal surface was lined by ciliated pseudostratified columnar epithelium with goblet cells resting on a well-defined basement membrane. Subepithelial connective tissue containing blood vessels was observed in the underlying lamina propria (Figure 1). Masson trichrome stained sections showed interconnected collagen fibres in the lamina propria (Figure 2).

Semithin sections clarified pseudostratified epithelium composed of ciliated columnar cells with rounded to oval nuclei and intervening more darkly stained cup shaped goblet cells. Basal cells appeared pyramidal with rounded nuclei and were observed resting on the basement membrane in-between other cells but not reaching the luminal surface (Figure 3).

Transmission electron microscopic ultrathin sections showed tall columnar cells with rounded to oval nuclei and many well defined regularly arranged cilia emerging from their apical luminal surface. Intervening neighboring flask shaped goblet cells were clearly identified from their neighboring ciliated columnar cells. The intervening goblet cells showed secretory granules (Figure 4).

Examination of tracheal sections of group II rats that were exposed to NaOCL inhalation revealed marked distortion of tracheal mucosal histoarchitecture. Epithelial lining showed regions composed of disorganized cells with darkly stained nuclei and some of which appeared with vacuolated cytoplasm. Many ciliated columnar cells also revealed amalgamation or loss of their apical cilia. Apparent increase in the number of goblet cells was also noted as compared to group I rats. Moreover, apparent increase in the content of mononuclear cellular infiltration and engorged blood vessels were encountered in the connective tissue of

the lamina propria in these regions (Figure 5). However, other regions appeared almost denuded of epithelial lining or lined by a single layer of cuboidal or flat cells with apparent degenerative changes in the lamina propria of those regions with few small, engorged blood vessels (Figure 6). Masson trichrome stained sections revealed massive deeply stained irregularly arranged collagen fibers with cellular infiltrates and dilated engorged blood vessels in the lamina propria of some regions (Figure 7). However, the regions with denuded epithelial lining showed some few collagen fibers with persistent cellular infiltrates (Figure 8).

Semithin sections revealed almost ununiform appearance of both ciliated columnar cells and the intervening goblet cells (Figure 9) compared to the control group. Ciliated columnar cells appeared variable in shape with indistinct cell boundaries between many of them (Figure 10). Their nuclei appeared variable in shape where some appeared oval, spindle shaped, and others were ghost like with ill-defined outline (Figure 11). Some had scarce apical cilia (Figure 9), others showed amalgamation of their cilia (Figure 10) and some others lost their apical cilia (Figure 12). Goblet cells revealed an apparent increase in their number with loss of their uniform cup shape as compared to group I (Figure 11). Cells with vacuolated cytoplasm were frequently observed in the lining epithelium (Figure 9). Moreover, some cells appeared ballooned with marked vacuolation of their cytoplasm (Figure 11). Areas of desquamated epithelium were also noticed (Figure 10). Basal cells appeared variable in shape (Figures 10,12) compared to those of the control group. Mononuclear cellular infiltrates were frequently observed in the lamina propria (Figure 10).

Electron microscopic examination further clarified the degenerative epithelial changes. Ciliated columnar cells were variable in shape, height, and nuclear morphology. Some were tall columnar with large irregular euchromatic nuclei (Figure 13). The cytoplasm of some cells contained cytoplasmic vacuoles (Figure 14). Some cells had indistinct cell boundaries in between (Figure 13). Moreover, some ciliated cells appeared small cuboidal with notable decrease in their height with small shrunken heterochromatic nuclei (Figure 15). Apical cilia appeared scarce (Figure 15) or even lost (Figure 16) in many cells. Some cells appeared with markedly vacuolated cytoplasm enclosing only an electron lucent nucleus (Figure 16). Goblet cells appeared variable in shape (Figure 16). Many basal cells appeared enlarged in size and irregular in shape (Figure 17). The lamina propria showed mononuclear cellular infiltrate, in which some showed irregular cellular processes and enclosed Kidney-shaped nucleus with peripheral chromatin condensation most probably resembling macrophage (Figure 15). Moreover, subepithelial dense collagen fibers were frequently observed in lamina propria (Figure 17).

Examination of sections of the recovery group showed that the tracheal lining was almost restored throughout its circumference. Yet, this reparative epithelium appeared disorganized showing relatively few intervening goblet cells, as compared to group II. Cilia were more or less restored but appeared amalgamated in some cells (Figure 18). However, it was also apparent that areas in proximity could be at different stages of repair process. Lamina propria appeared containing dense connective tissue with few mononuclear cellular infiltrations. Few congested blood vessels were still encountered as compared to group II (Figure 18). Masson's trichrome stained sections further revealed condensation of deeply stained collagen fibers with mononuclear cellular infiltration in the lamina propria (Figure 19).

Semithin sections revealed reparative epithelium with no loss of its continuity. Most of the ciliated columnar cells regained their basal oval nuclei (Figure 20) however, others showed vacuolation in their cytoplasm (Figure 21). Well defined apical cilia were evident in many of them (Figure 20) however only few cells showed loss of their cilia (fFigure 21). Goblet cells almost regained their cup shaped appearance (Figure 20). Some basal cells were mostly pyramidal in shape (Figure 20).

Electron microscopic examination showed hypercellularity in the regenerative epithelium (Figure 22). Ciliated columnar cells had variable shaped nuclei where some were almost oval euchromatic, others had irregular outline with patchy chromatin, and few appeared with shrunken nuclei (Figure 22). Restoration of apical cilia was observed in most columnar cells (Figure 23). Goblet cells still exhibited variable shape and some of their nuclei were almost oval, while others appeared irregular (Figure 23). Basal cells appeared with variable shaped nuclei (Figure 22). Moreover, dense collagen fibers were still observed in the lamina propria (Figures 22,23).

Statistical Results (Table & Histogram1)

Statistical analysis of the morphometric results of the present study showed that the tracheal epithelium of the rats that were exposed to NaOCL inhalation in group II had highly significant decrease ($P < 0.001$) in their mean epithelial height together with highly significant increase ($P < 0.001$) in the mean number of their goblet cells as compared to the control group (Histograms 1A,1B respectively). Moreover, a highly significant increase ($P < 0.001$) in mean area percentage of collagen in lamina propria was detected compared to the control group (Histogram 1C).

On the other hand, tracheal epithelium of rats of the recovery group revealed significant increase ($P < 0.05$) in the mean epithelial height as compared to group II, however, it was still significantly decreased ($P < 0.05$) when compared to the control group (Histogram 1A). Mean goblet cell number of the recovery group showed highly significant decrease ($P < 0.001$) in comparison to group II (Histogram 1B) and was almost back to the normal control level where non-significant changes ($P > 0.05$) were noted when it was compared to the group I. However, persistent increase in the mean area percentage of collagen was noted in the recovery group where its comparison with group II showed non-significant results ($P > 0.05$) while its comparison with the control group still revealed highly significant increase ($P < 0.001$) (Histogram 1C).

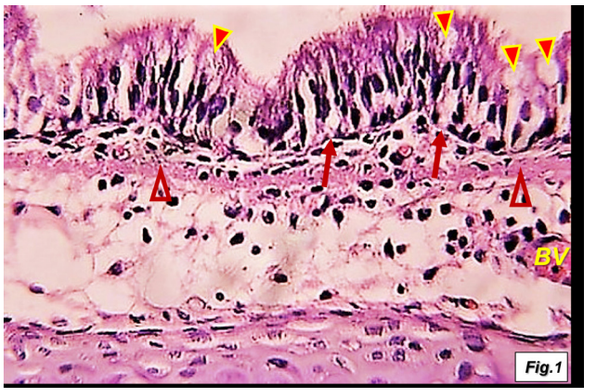

Fig. 1: showing pseudostratified columnar ciliated epithelium with goblet cells (▲) resting on a basement membrane (↑). Notice the connective tissue fibers (Δ) and blood vessel (BV) in the lamina propria. (Group I, Hx.&E.x400)

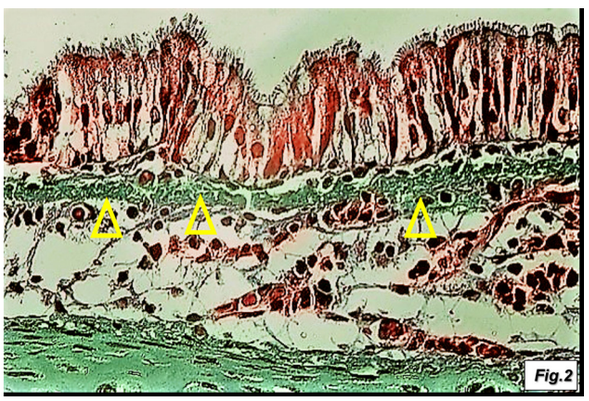

Fig. 2: showing fine collagen fibres (Δ) in the lamina propria. (Group I, Masson`s Trichrome x400)

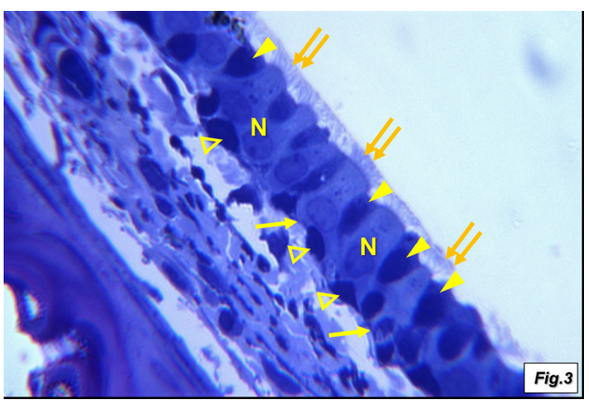

Fig. 3: showing columnar ciliated cells with rounded nuclei (N) and apical cilia (↑↑) and intervening darkly stained cup shaped goblet cells (▲). Notice the pyramidal basal cells with rounded nuclei (Δ) resting on the basement membrane (↑). (Group I, Toluidine blue, x1000)

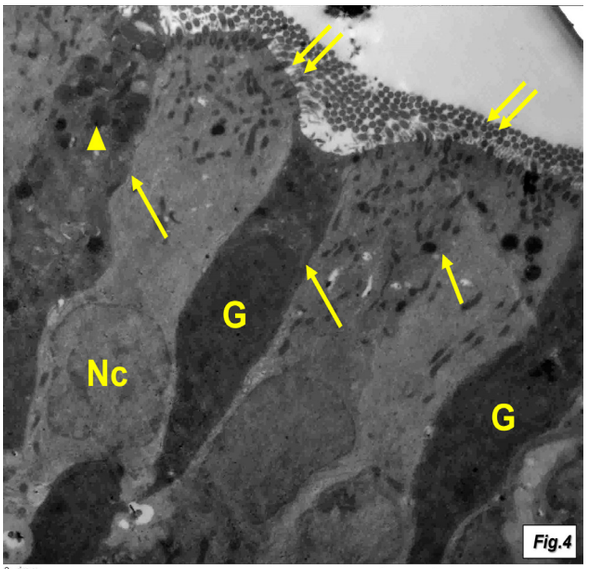

Fig. 4: showing columnar cells with rounded to oval nuclei (Nc) and intervening darkly stained flask shaped goblet cells (G). Notice the regularly arranged cilia (↑↑) emerging from the luminal surface of ciliated cells and the secretory granules (▲) in goblet cell. Note also the clear demarcation between cells (↑). (Group I, Uranyl acetate & lead citrate x1500)

Fig. 5: showing disorganized cells with darkly stained nuclei (red▲), some of which appeared with vacuolated cytoplasm (Δ) and some ciliated cells show amalgamation (↑↑) or loss of their apical cilia (↑) Notice the apparent increase in goblet cells (yellow ▲). Note also the connective tissue with cellular infiltration (*) and engorged blood vessels (BV) in the lamina propria. (Group II, Hx.&E.x400).

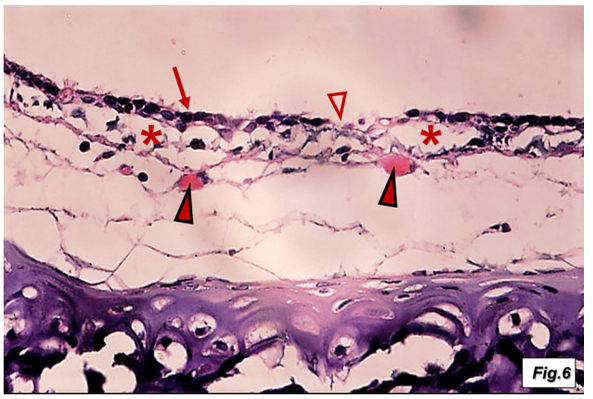

Fig. 6: showing mucosa with single layer of cuboidal to flat cells (↑) with an area almost denuded of epithelium (Δ). Notice the degenerated lamina propria (*) with small engorged blood vessels (▲). (Group II, Hx.&E. x400)

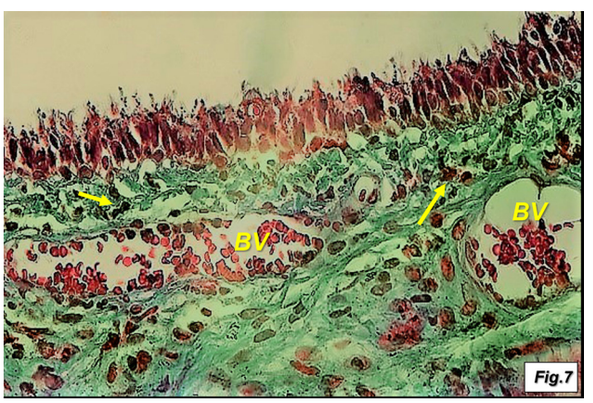

Fig. 7: showing deeply stained collagen fibers with cellular infiltrates (↑) and dilated engorged blood vessels (BV) in the lamina propria. (Group II, Masson`s Trichrome x400)

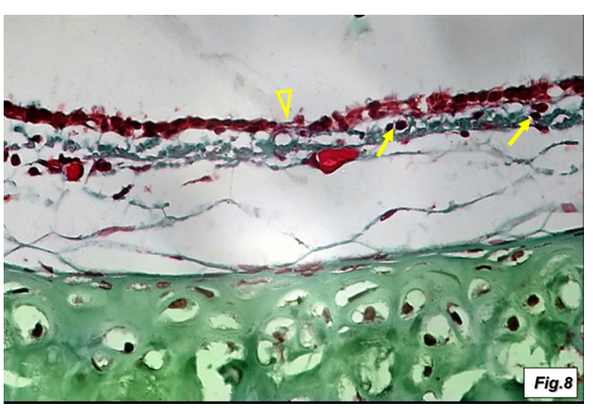

Fig. 8: showing an area with denuded epithelium (Δ) and few subepithelial collagen fibers with some cellular infiltrates (↑). (Group II, Masson`s Trichrome x400)

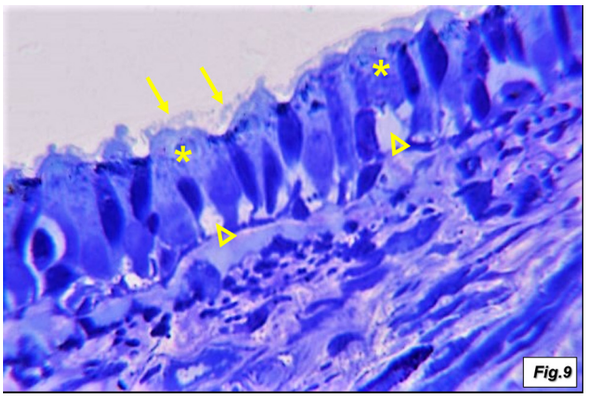

Fig. 9: showing ununiform appearance of both ciliated columnar cells and the intervening goblet cells. Notice the variable shaped ciliated cells (*) with cytoplasmic vacuolation (Δ) in some of them. Note also the scarce apical cilia (↑) of ciliated cells. (Group II, Toluidine blue, x1000)

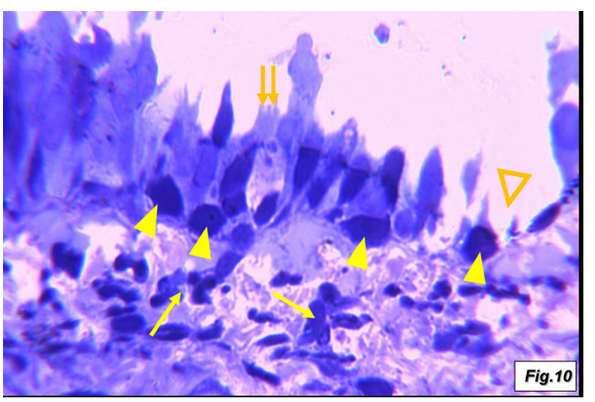

Fig. 10: showing ciliated cells with indistinct cell boundaries with some amalgamated cilia (↑↑). Notice the areas of desquamated epithelium (Δ) and the disorganized basal cells (▲). Note also the mononuclear cellular infiltrates (↑) in the lamina propria. (Group II, Toluidine blue, x1000)

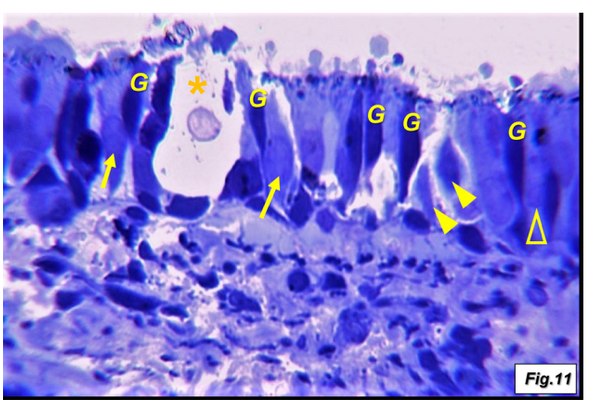

Fig. 11: showing ciliated cells with oval (↑) , spindle shaped (▲), and ill-defined outlined (Δ) nuclei. Notice the apparent increase in the number of goblet cells (G) with loss of their uniform cup shape. Note also the ballooned cell (*) with markedly vacuolated cytoplasm. (Group II, Toluidine blue, x1000)

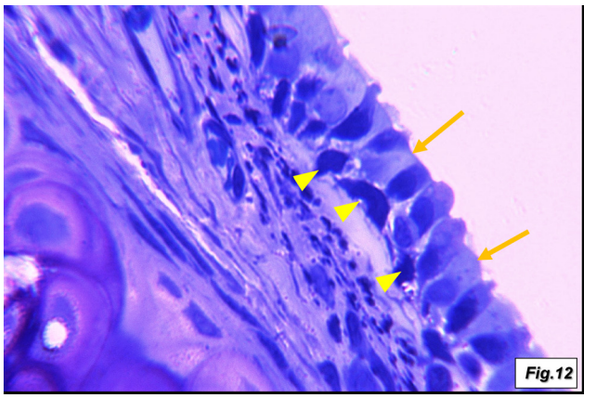

Fig. 12: Showing ciliated cells with loss of their apical cilia (↑). Notice the variable shaped basal cells (▲). (↑). (Group II, Toluidine blue, x1000)

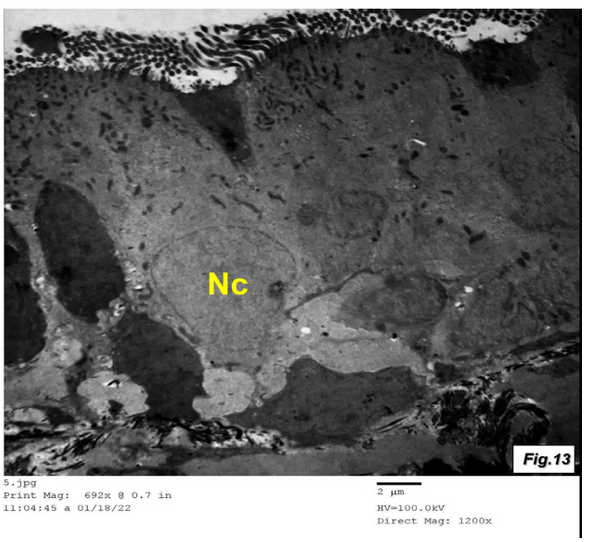

Fig. 13: showing tall columnar ciliated cells with indistinct cell boundaries. Notice the large irregular euochromatic nucleus (Nc). (Group II, Uranyl acetate & lead citrate x1200)

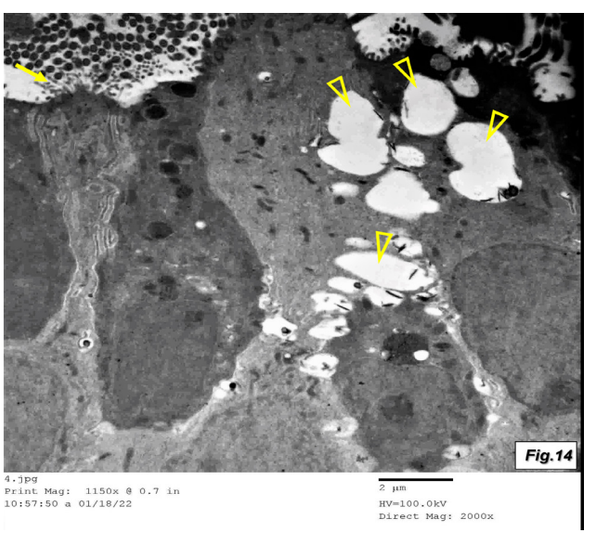

Fig. 14: showing ciliated cell with cytoplasmic vacuoles (Δ). (Group II, Uranyl acetate & lead citrate x2000)

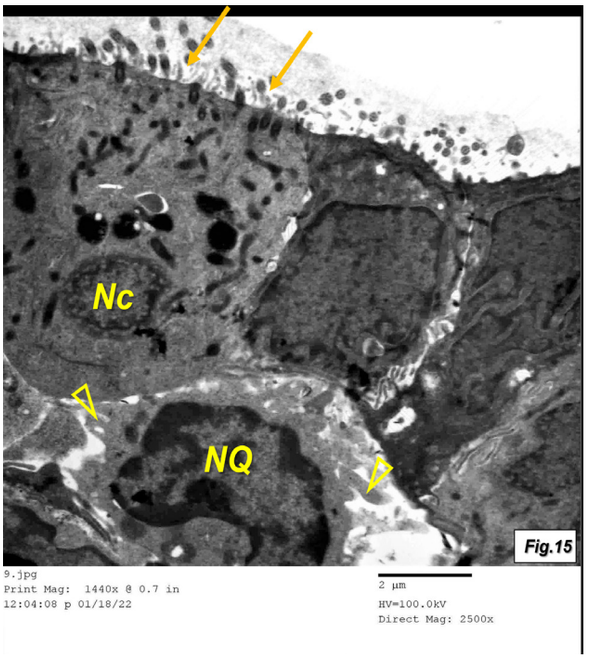

Fig. 15: showing short cuboidal ciliated cell with shrunken heterochromatic nucleus (Nc) and scarce cilia (↑). Note also the mononuclear cell with irregular cytoplasmic cellular processes (Δ) and enclosing a kidney-shaped nucleus (NQ) with peripheral chromatin condensation. (Group II, Uranyl acetate & lead citrate x2500)

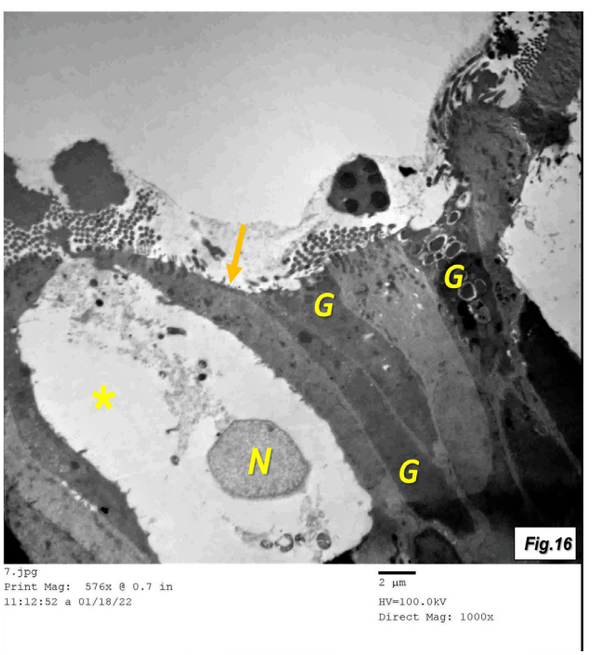

Fig. 16: showing variable shaped goblet cells (G). Notice the ciliated cell with almost totally vacuolated cytoplasm (*) enclosing only an electron lucent nucleus (N). Notice the loss of cilia (↑). (Group II, Uranyl acetate & lead citrate x1000)

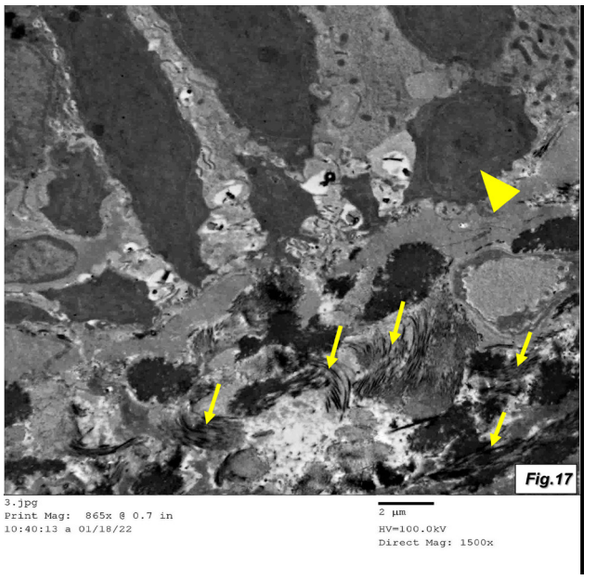

Fig. 17: showing enlarged irregular basal cell (▲). Notice the subepithelial collagen fibers (↑). (Group II, Uranyl acetate & lead citrate x1500)

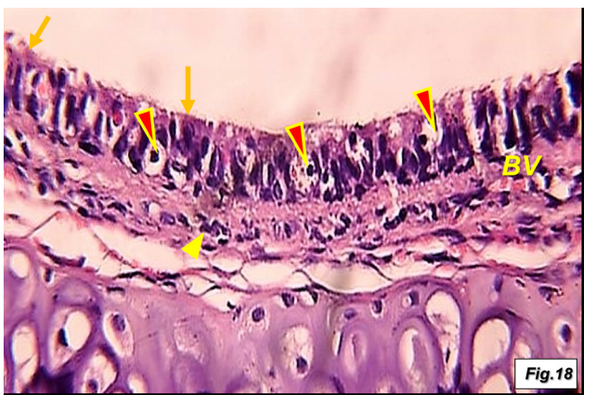

Fig. 18: A photomicrograph of trachea of recovery group (group III) showing disorganized reparative epithelium with intervening goblet cells (red▲). Notice the restored yet amalgamated cilia (↑). Note also the dense connective tissue (*) with cellular infiltrates (yellow▲) and the small congested blood vessel (BV) in the lamina propria. (Group II, Hx.&E.x400)

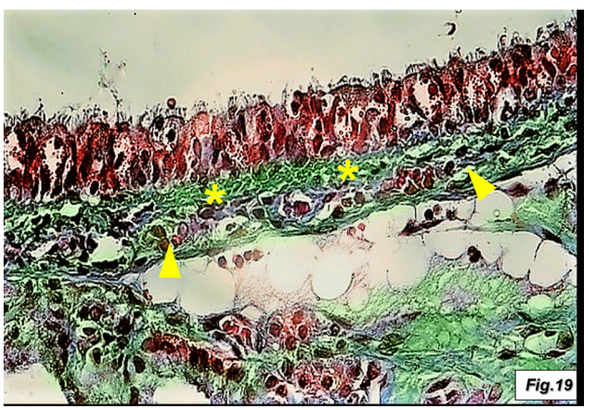

Fig. 19: A photomicrograph of trachea of recovery group (group III) showing dense collagen fibers (*) with cellular infiltrates (▲) in the lamina propria. (Group III, Masson`s Trichrome x400)

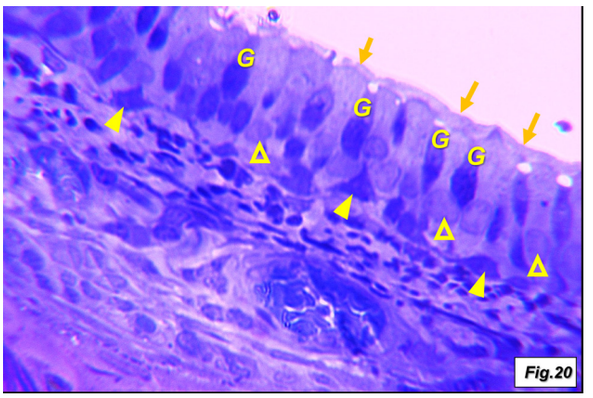

Fig. 20: showing ciliated cells with basal oval nuclei (Δ) and well defined apical cilia (↑) and the cup shaped goblet cells (G). Note also the Basal cells (▲) which are mostly pyramidal in shape. (Group II, Toluidine blue, x1000)

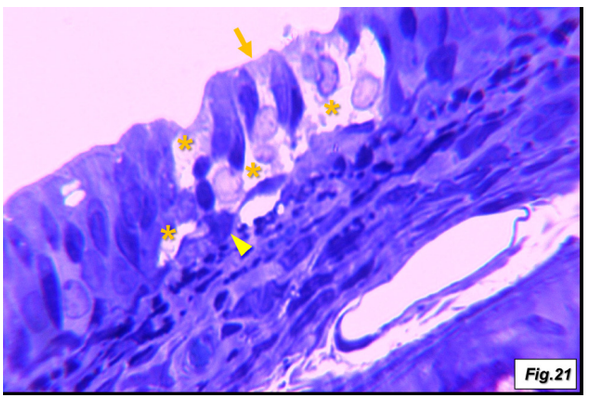

Fig. 21: showing ciliated cells appeared with marked cytoplasmic vacuolation (*) and loss of cilia (↑). (Group III, Toluidine blue, x1000)

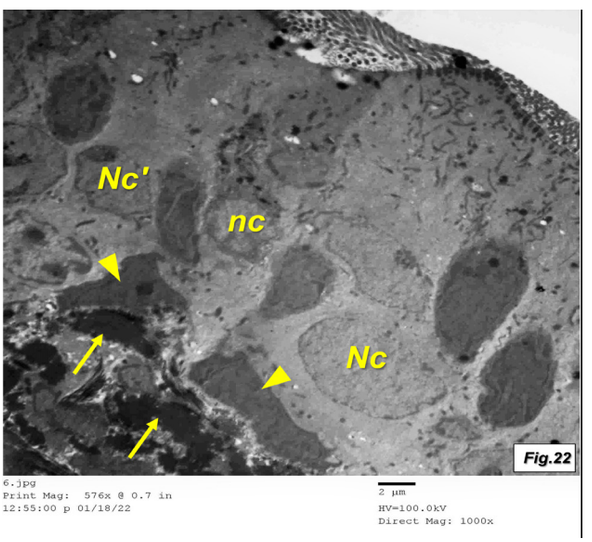

Fig. 22: showing hypercellularity of epithelial cells with indistinct cell boundaries. Notice the oval euchromatic nucleus (Nc), the irregularly outlined nucleus with patchy chromatin (Nc') and the shrunken nucleus (nc) of ciliated cells. Note also the variable shaped basal cells (▲) and the collagen fibers (↑) in the lamina propria. (Group III, Uranyl acetate & lead citrate x1000)

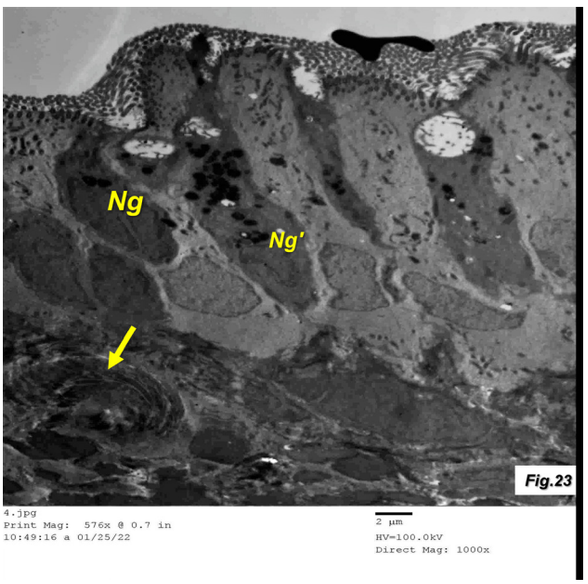

Fig. 23: showing goblet cells with almost oval nuclei (Ng) and others having irregular ones (Ng'). Notice the apical cilia (↑↑) in ciliated cells and the dense collagen fibers (↑) in the lamina propria. (Group III, Uranyl acetate & lead citrate x1000)

Table 1: Showing mean epithelial height, mean number of goblet cells and mean area percentage of collagen done by (student "t" test)

		Group I (Control Group	Group II (Sodium Hypochlorite Inhalation Group)	Group III (Recovery Group)
	Mean Epithelial Height (in µm)	31.63 ±0.84	14.53 ±6.59	25.74 ±3.65
T test	Between Group I&II		P= 0.000088 ($P < 0.001^{**}$)	
T test	Between Group II&III		P= 0.0045 ($P < 0.05^{*}$)	
T test	Between Group I&III		P= 0.0032 ($P < 0.05^{*}$)	
	Mean Goblet Cell Number	3.83 ±0.75	7.5 ±1.05	2.83 ±1.17
T test	Between Group I&II		P= 0.000039 ($P < 0.001^{**}$)	
T test	Between Group II&III		P= 0.000027 ($P < 0.001^{**}$)	
T test	Between Group I&III		P= 0.11 ($P > 0.05^{\phi}$)	
	Mean Area Percentage of Collagen (%)	38.63 ±1.76	64.26 ±7.6	57.97 ±1.94
T test	Between Group I&II		P= 0.000011 ($P < 0.001^{**}$)	
T test	Between Group II&III		P= 0.078 ($P > 0.05^{\phi}$)	
T test	Between Group I&III		P= 0.000057 ($P < 0.001^{**}$)	

Values are expressed as Mean ± SD. (**= Highly Significant, * = Significant and ϕ = non-significant)

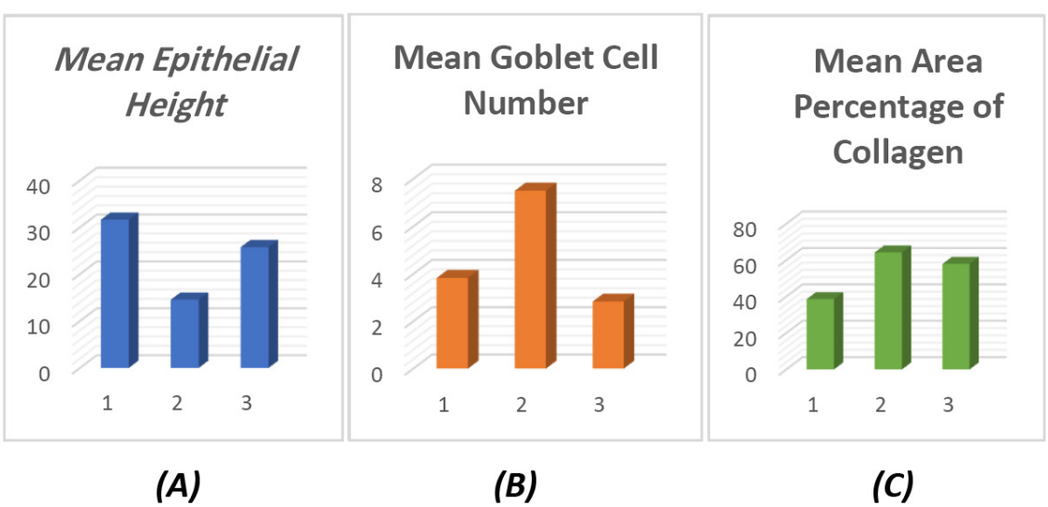

Histogram 1: demonstrating the morphometric comparison between the three groups as regards; (A) mean epithelial height, (B) mean goblet cell number and (C) mean area percentage of collagen.

DISCUSSION

As an attempt to stop the COVID-19 ongoing outbreak and control this pandemic, various household disinfectants and preventive measures competing contamination have become part of our lives in the past couple of years[13]. Among these disinfectants is NaOCL, whose usage has greatly affected the respiratory system ranging from mild airways dysfunction up to acute lung injury with probable mortality[10]. Therefore, this study focused on the histopathological effects of NaOCL on the trachea as a crucial part of the upper respiratory tract.

Results of examination of tracheal sections of rats exposed to NaOCL inhalation in the current study showed marked distortion of the mucosal histoarchitecture. Epithelial lining revealed highly significant decrease ($P < 0.001$) in height compared to the control group and was composed of disorganized ciliated and intervening goblet cells compared to the control group.

Ciliated columnar cells revealed marked distortion of their apical cilia where some cells had scarce cilia, others had loss of cilia in addition to amalgamation of cilia in some others. Similarly, it has been previously reported that the trachea of animals subjected to inhalation of chlorine containing detergents, revealed disruption of the tissue with decrease in epithelial height, increase in goblet cell number and absence of cilia. Moreover, ciliary amalgamation was considered as a sign of epithelial disruption which could be attributed to the reported hyperplasia of mucus-secreting submucosal glands that negatively affected the airway clearance mechanisms[14,15].

Moreover, some ciliated columnar cells appeared ballooned with almost totally vacuolated cytoplasm enclosing a nucleus. These degenerative signs could be attributed to the reported data that chlorine is a highly unstable molecule[16] and when inhaled, it reacts with the water content on the moist surface of the respiratory airways with subsequent formation of oxygen free radicals leading to marked upper and lower respiratory tract insults[17,18].

Additionally, the generation of these oxygen free radicals was the most probable cause for the highly significant increase ($P < 0.001$) in goblet cell number noted in group II when compared to the control group. Marked increase in goblet cell number is a common response to a variety of airway insults and oxidative stress mediators, among which are cigarette smoking, exposure to irritant gases, inflammatory mediators, and chronic obstructive pulmonary diseases[19,20,21]. This increase in number is associated with increased MUC gene expression responsible for mucin production with subsequent increase in mucin secretion[22,23].

Moreover, oxygen free radicals also target and damage proteins and lipid compounds, and causes hardening of cell membranes, which are made of unsaturated fat. This hardening leads to loss of the cellular ability to receive nutrients and ending up eventually in cell death[16]. This could explain the areas of desquamation and sloughing of epithelial cells noted in group II where some areas appeared almost completely denuded of the epithelial lining. It has been similarly reported that high-level chlorine exposure results in sloughing of the pseudostratified airway respiratory epithelium of the proximal airways[7,24,25].

However, other neighboring areas in group II appeared to be lined by a single layer of cuboidal to flat cells. This could be explained by a previous study which declared that; with the loss of most epithelial cells after chlorine injury, basal cells were the only surviving cells initially observed in the trachea as a thin layer of flattened epithelial cells that served to repopulate the trachea[26].

Regarding the tracheal lamina propria of rats of this group, many regions revealed apparent increase in collagen fibers with mononuclear cellular infiltrates and dilated engorged blood vessels. This was further documented by the highly significant increase ($P < 0.001$) in the mean area percentage of collagen in group II as compared to control group. Similarly, it has been also reported that exposure to chlorine inhalation, led to inflammatory cell infiltration with marked collagen deposition in lung tissue with subsequent fibrosis[5,27,28].

Although the airway epithelium was the first target of inhaled chlorine gas causing its direct oxidative injury, however, further oxidative damage resulted in migration and infiltration of inflammatory cells, such as neutrophils, into the airway mucosa with subsequent release of inflammatory cytokines and proteolytic enzymes leading to airway hyper-responsiveness[29,30,31].

On the other hand, examination of trachea of rats of the recovery group revealed restoration of the continuity of epithelial lining with no more sloughing or desquamation. Mean epithelial height was significantly increased ($P < 0.05$) compared to group II however, it was still not yet back to the normal control levels where significant decrease ($P < 0.05$) was noted when it was compared to the control group measurements. Moreover, the epithelium appeared disorganized with indistinct cell boundaries. This finding was in accordance with a study which reported that the initial regenerated epithelium following chlorine exposure showed an abnormal distribution of epithelial cells. This chlorine induced structural epithelial changes could potentially impair airway epithelial-related functions such as response to subsequent injury[32,33].

Regarding the cells of regenerative epithelium of the recovery group, ciliated columnar cells almost regained their basal rounded nuclei apart from few others still showing vacuolation. Moreover, their apical cilia were almost well defined in many of them and scarce or amalgamated in few of them. Goblet cells showed highly significant decrease ($P < 0.001$) in their mean number compared to group II and revealed almost back ($P > 0.05$) to the normal control range. These cells almost regained their cup shaped appearance. It has been reported that cessation of exposure to the irritant or causative insult leads

to recovery with a decrease of goblet cell number which is accomplished by certain extracellular and intracellular signaling molecules[22].

Moreover, basal cells were still variable in shape. Basal cells, the principal airway stem cells, are the ones responsible for tracheal epithelial regeneration. After injury, they proliferate and differentiate to other cell types including goblet and ciliated cells to rebuild up the airway epithelium[26,34]. However, the chance of fibrosis increases if the number of these cells was inadequate to re-establish the epithelium before the development of a fibrotic scar[32]. Thus, basal cells affection could also be one of the leading causes of the persistent deposition of collagen fibers in this recovery group which was further proven by the persistent increase in the mean area percentage of collagen where its comparison with group II showed non-significant results ($P > 0.05$) and its comparison with the control group still revealed highly significant increase ($P < 0.001$).

Although the initial development of fibrosis is dependent on inflammation however, it's worth mentioning that further pro-fibrotic processes become self-sustaining and can proceed in the absence of continued inflammation[32]. This could further explain the incomplete tracheal recovery and the persistent fibrotic changes noted in this study despite the cessation of exposure which could lead to permanent tracheal insult. This may further clarify what was previously stated regarding chlorine inhalation which has been stated to result not only in acute lung injury but also in long-lasting irreversible respiratory insult[35].

CONCLUSION

Sodium hypochlorite inhalation has been found to cause partially reversible histopathological effects on the tracheal mucosa. Thus, excessive use of household chlorine containing detergents should be limited or better substituted by other non-injurious substances.

STUDY LIMITATIONS

A longer period for recovery could have been more conclusive of the possibility of complete reversibility of NaOCL induced histopathological effects.

RECOMMENDATIONS

Future studies with longer duration of recovery are recommended. Additional histological techniques would be of great value.

CONFLICT OF INTERESTS

There are no conflicts of interest.

REFERENCES

1. Al-Sayah MH: Chemical disinfectants of COVID-19: an overview. J Water Health. (2020) Oct;18(5):843-848. doi: 10.2166/wh.2020.108. PMID: 33095205.
2. Cheng VCC, Wong SC, Chen JHK, Yip CCY, Chuang VWM, Tsang OTY, Sridhar S, Chan JFW, Ho PL and Yuen KY: Escalating infection control response to the rapidly evolving epidemiology of the coronavirus disease 2019 (COVID-19) due to SARS-CoV-2 in Hong Kong. Infect Control Hosp Epidemiol. (2020) May;41(5):493-498. doi: 10.1017/ice.2020.58. Epub 2020 Mar 5. PMID: 32131908; PMCID: PMC7137535.
3. Kampf G, Todt D, Pfaender S and Steinmann E: Persistence of coronaviruses on inanimate surfaces and their inactivation with biocidal agents. J Hosp Infect. (2020) Mar;104(3):246-251. doi: 10.1016/j.jhin.2020.01.022. Epub 2020 Feb 6. Erratum in: J Hosp Infect. 2020 Jun 17;: PMID: 32035997; PMCID: PMC7132493.
4. Pereira SS, Oliveira HM, Turrini RN and Lacerda RA: Disinfection with sodium hypochlorite in hospital environmental surfaces in the reduction of contamination and infection prevention: a systematic review. Rev Esc Enferm USP. (2015) Aug;49(4):681-688. Portuguese. doi: 10.1590/S0080-623420150000400020. PMID: 26353107.
5. Aboul-Fotouh S and Farouk GM: Mitigation of Delayed Sodium Hypochlorite-Induced Lung Injury by Phosphodiesterase Enzyme Inhibitors (PDEIs), Pentoxifylline and Theophylline, in Guinea Pigs. Egyptian Journal of Basic and Clinical Pharmacology (2011) 1(1): 9-21.
6. Winder C: The toxicology of chlorine. Environ Res. (2001) Feb;85(2):105-114. doi: 10.1006/enrs.2000.4110. PMID: 11161660.
7. Leustik M, Doran S, Bracher A, Williams S, Squadrito GL, Schoeb TR, Postlethwait E and Matalon S: Mitigation of chlorine-induced lung injury by low-molecular-weight antioxidants. Am J Physiol Lung Cell Mol Physiol. (2008) Nov;295(5):L733-743. doi: 10.1152/ajplung.90240.2008. Epub 2008 Aug 15. PMID: 18708632; PMCID: PMC2584876.
8. Bruch MK: Toxicity and safety of topical sodium hypochlorite. Contrib Nephrol. (2007);154:24-38. doi: 10.1159/000096812. PMID: 17099299.
9. Weisel CP, Richardson SD, Nemery B, Aggazzotti G, Baraldi E, Blatchley ER 3rd, Blount BC, Carlsen KH, Eggleston PA, Frimmel FH, Goodman M, Gordon G, Grinshpun SA, Heederik D, Kogevinas M, LaKind JS, Nieuwenhuijsen MJ, Piper FC and Sattar SA: Childhood asthma and environmental exposures at swimming pools: state of the science and research recommendations. Environ Health Perspect. (2009) Apr;117(4):500-507. doi: 10.1289/ehp.11513. Epub 2008 Sep 30. PMID: 19440486; PMCID: PMC2679591.
10. White CW and Martin JG: Chlorine gas inhalation: human clinical evidence of toxicity and experience in animal models. Proc Am Thorac Soc. (2010) Jul;7(4):257-63. doi: 10.1513/pats.201001-008SM. PMID: 20601629; PMCID: PMC3136961.

11. Bancroft JD and Layton C: The Hematoxylin and eosin. In: Suvarna SK, Layton C and Bancroft JD editors. Theory & Practice of histological techniques. 7th ed., Churchill Livingstone of El Sevier. Philadelphia. Ch. (2013)10 to 18. 172 - 426.
12. Graham L and Orenstein JM: Processing tissue and cells for transmission electron microscopy in diagnostic pathology and research. Nat Protoc. (2007);2(10):2439-50. doi: 10.1038/nprot.2007.304. PMID: 17947985; PMCID: PMC7086545.
13. Shimabukuro PMS, Duarte ML, Imoto AM, Atallah ÁN, Franco ESB, Peccin MS and Taminato M: Environmental cleaning to prevent COVID-19 infection. A rapid systematic review. Sao Paulo Med J. (2020) Nov-Dec;138(6):505-514. doi: 10.1590/1516-3180.2020.0417.09092020. PMID: 33206913.
14. Vaezi GH, Aliabadi F, shiravi AB, pourkazem M and Toosi F: Histopathology of Inhalation of Industrial Bleach and Detergent Mixture on Epithelial Layer of Trachea in Mice. Journal of Chemical Health Risks (2011) 1(1): 29-33.
15. Ziad AS and Hossam NN: Histological Changes in Tissues of Trachea and Lung Alveoli of Albino Rats Exposed to the Smoke of Two Types of Narghile Tobacco Products, Jordan Journal of Biological Sciences (2011) volume 4, 219-224.
16. Han D, Williams E and Cadenas E: Mitochondrial respiratory chain-dependent generation of superoxide anion and its release into the intermembrane space. Biochem J. (2001) Jan 15;353(Pt 2):411-416. doi: 10.1042/0264-6021:3530411. PMID: 11139407; PMCID: PMC1221585.
17. Muller F: The nature and mechanism of superoxide production by the electron transport chain: Its relevance to aging. J Am Aging Assoc. (2000) Oct;23(4):227-53. doi: 10.1007/s11357-000-0022-9. PMID: 23604868; PMCID: PMC3455268.
18. Gorguner M, Aslan S, Inandi T and Cakir Z: Reactive airways dysfunction syndrome in housewives due to a bleach-hydrochloric acid mixture. Inhal Toxicol. (2004) Feb;16(2):87-91. doi: 10.1080/08958370490265004. PMID: 15204781.
19. Rogers DF: Airway goblet cells: responsive and adaptable front-line defenders. Eur Respir J. (1994) Sep;7(9):1690-706. PMID: 7995400.
20. Nadel JA and Burgel PR: The role of epidermal growth factor in mucus production. Curr Opin Pharmacol. (2001) Jun;1(3):254-8. doi: 10.1016/s1471-4892(01)00045-5. PMID: 11712748.
21. Huang X, Guan W, Xiang B, Wang W, Xie Y, Zheng J. MUC5B regulates goblet cell differentiation and reduces inflammation in a murine COPD model. Respir Res. 2022 Jan 18;23(1):11. doi: 10.1186/s12931-021-01920-8. PMID: 35042537; PMCID: PMC8764756.
22. Rogers DF: Cells in focus. The airway goblet cell. The International Journal of Biochemistry & Cell Biology (2003) (35) 1–6.
23. Galante CM. Asthma management updates. Nursing. 2022 Feb 1;52(2):25-34. doi: 10.1097/01.NURSE.0000806156.52958.3c. PMID: 35085192.
24. Tian X, Tao H, Brisolara J, Chen J, Rando RJ and Hoyle GW: Acute lung injury induced by chlorine inhalation in C57BL/6 and FVB/N mice. Inhal Toxicol. (2008) Jul;20(9):783-93. doi: 10.1080/08958370802007841. PMID: 18645717.
25. Tuck SA, Ramos-Barbón D, Campbell H, McGovern T, Karmouty-Quintana H and Martin JG. Time course of airway remodelling after an acute chlorine gas exposure in mice. Respir Res. (2008) Aug 14;9(1):61. doi: 10.1186/1465-9921-9-61. PMID: 18702818; PMCID: PMC2531104.
26. Musah S, Chen J and Hoyle GW: Repair of tracheal epithelium by basal cells after chlorine-induced injury. Respir Res. (2012) Nov 22;13(1):107. doi: 10.1186/1465-9921-13-107. PMID: 23170909; PMCID: PMC3544626.
27. Lederer DJ and Martinez FJ: Idiopathic Pulmonary Fibrosis. N Engl J Med. (2018) May 10;378(19):1811-1823. doi: 10.1056/NEJMra1705751. PMID: 29742380.
28. Mulugeta S, Nureki S and Beers MF: Lost after translation: insights from pulmonary surfactant for understanding the role of alveolar epithelial dysfunction and cellular quality control in fibrotic lung disease. Am J Physiol Lung Cell Mol Physiol. (2015) Sep 15;309(6):L507-25. doi: 10.1152/ajplung.00139.2015. Epub 2015 Jul 17. PMID: 26186947; PMCID: PMC4572416.
29. Martin JG, Campbell HR, Iijima H, Gautrin D, Malo JL, Eidelman DH, Hamid Q and Maghni K: Chlorine-induced injury to the airways in mice. Am J Respir Crit Care Med. (2003) Sep 1;168(5):568-74. doi: 10.1164/rccm.200201-021OC. Epub 2003 Apr 30. PMID: 12724121.
30. Yadav AK, Doran SF, Samal AA, Sharma R, Vedagiri K, Postlethwait EM, Squadrito GL, Fanucchi MV, Roberts LJ 2nd, Patel RP and Matalon S: Mitigation of chlorine gas lung injury in rats by postexposure administration of sodium nitrite. Am J Physiol Lung Cell Mol Physiol. (2011) Mar;300(3):L362-9. doi: 10.1152/ajplung.00278.2010. Epub 2010 Dec 10. PMID: 21148791; PMCID: PMC3064287.
31. Puissant B, Barreau C, Bourin P, Clavel C, Corre J, Bousquet C, Taureau C, Cousin B, Abbal M, Laharrague P, Penicaud L, Casteilla L and Blancher A: Immunomodulatory effect of human adipose tissue-derived adult stem cells: comparison with bone marrow mesenchymal stem cells. Br J Haematol. (2005) Apr;129(1):118-29. doi: 10.1111/j.1365-2141.2005.05409.x. PMID: 15801964.

32. Musah S, Chen J, Schlueter C, Humphrey DM Jr, Stocke K, Hoyle MI and Hoyle GW: Inhibition of chlorine-induced airway fibrosis by budesonide. Toxicol Appl Pharmacol. (2019) Jan 15;363:11-21. doi: 10.1016/j.taap.2018.08.024. Epub 2018 Sep 3. PMID: 30189237; PMCID: PMC6342561.

33. Mo Y, Chen J, Humphrey DM Jr, Fodah RA, Warawa JM and Hoyle GW: Abnormal epithelial structure and chronic lung inflammation after repair of chlorine-induced airway injury. Am J Physiol Lung Cell Mol Physiol. (2015) Jan 15;308(2):L168-78. doi: 10.1152/ajplung.00226.2014. Epub 2014 Nov 14. PMID: 25398987; PMCID: PMC4338946.

34. Davis JD, Wypych TP. Cellular and functional heterogeneity of the airway epithelium. Mucosal Immunol. 2021 Sep;14(5):978-990. doi: 10.1038/s41385-020-00370-7. Epub 2021 Feb 19. Erratum in: Mucosal Immunol. 2022 Mar 16;: PMID: 33608655; PMCID: PMC7893625.

35. Hoyle GW, Chen J, Schlueter CF, Mo Y, Humphrey DM Jr, Rawson G, Niño JA and Carson KH: Development and assessment of countermeasure formulations for treatment of lung injury induced by chlorine inhalation. Toxicol Appl Pharmacol. (2016) May 1;298:9-18. doi: 10.1016/j.taap.2016.03.001. Epub 2016 Mar 4. PMID: 26952014; PMCID: PMC4821717.

الملخص العربى

تأثير استنشاق هيبوكلوريت الصوديوم على تركيب الغشاء المخاطي للقصبة الهوائية في ذكور الجرذان البيضاء البالغة وإمكانية التعافي

ماري رفعت اسحق، هاجر يسري راضي و شيرين عادل سعد

قسم التشريح ، كلية الطب ، جامعة عين شمس

المقدمه: لقد أدى الوباء العالمي (COVID-١٩) إلى استخدام المطهرات مثل هيبوكلوريت الصوديوم على نطاق واسع. و قد صرحت بعض الدراسات أن التعرض للمطهرات التي تحتوي على الكلور يعتبر مصدرا لتهيج والتهاب في مجرى الهواء.

الهدف من هذه الدراسة: هو تحديد التأثيرات النسيجية المرضية لاستنشاق هيبوكلوريت الصوديوم على الغشاء المخاطي للقصبة الهوائية وامكانية اختفاء هذه التأثيرات عند الإستشفاء.

الطرق و المواد المستخدمه: تم استخدام اربعون من ذكور الجرذان البيضاء ، وقسمت الحيوانات إلى ثلاث مجموعات علي النحو التالي:

- المجموعة الأولى: و قد قسمت إلي مجموعتين تحتوي كل منهما علي عشرة جرذان هما:
- المجموعة IA: استخدمت كعنصر ظبط سلبي.
- المجموعة IB: تعرضت الجرذان لرذاذ من الماء المقطر لمدة ٢٠ دقيقة يوميا لمدة ثلاثة أسابيع.
- المجموعة الثانية: شملت عشرة جرذان و قد تعرضت لرذاذ ٤٪ هيبوكلوريت الصوديوم لمدة ٢٠ دقيقة يوميا لمدة ثلاثة أسابيع.
- المجموعة الثالثة: شملت عشرة جرذان و قد تعرضت لرذاذ ٤٪ هيبوكلوريت الصوديوم لمدة ٢٠ دقيقة يوميا مثل المجموعة السابقة ثم تُركت لمدة ثلاثة أسابيع أخرى دون تعرض.

بعد إنتهاء التجربة لكل مجموعة، تم تخدير الجرذان ثم التضحية بهم و استئصال القصبة الهوائية ومعالجتها للفحص بالمجهرين الضوئي والإلكتروني بالإضافة الي التحليل المورفومتري و الإحصائي.

النتائج: أظهر فحص عينات المجموعة الثانية للجرذان تشوهًا ملحوظًا في الخلايا الظهارية للقصبة الهوائية منها عدم وضوح للحدود ما بين الخلايا، وجود أنوية متقلصة متغايرة اللون وترقق أو فقدان شبه كامل للأهداب القمية . كما لوحظ ان هناك انخفاضا كبيرا في متوسط ارتفاع الظهارة مع زيادة كبيرة في كل من متوسط عدد الخلايا الكأسية ومتوسط النسبة المئوية لمساحة الكولاجين. أما عينات المجموعة الثالثة فقد أظهرت أن بطانة القصبة الهوائية قد تم ترميمها تقريبًا إلا أنها قد بدت غير منظمة كما تم إستعادة الأهداب إلا أنها كانت شبه مدمجة. عادت الخلايا الكأسية إلى متوسط العدد الطبيعي لكنها لا تزال متغايرة الشكل. أما بالنسبة لمتوسط إرتفاع الظهارة ومتوسط النسبة المئوية لمساحة الكولاجين فلم يعودا إلى معدلات التحكم الخاصة بهما.

الخلاصه: لقد أدي استنشاق هيبوكلوريت الصوديوم إلي تأثيرات نسيجية مرضية في الغشاء المخاطي للقصبة الهوائية و قد كانت هذه التأثيرات قابلة للعكس جزئيا فقط. لذلك ينصح بتجنب الإستخدام المفرط للمنظفات التي تحتوي علي الكلور و يفضل استبدالها بأخري.